Prelimbic neuron calcium activity predicts perceived hedonic value across drinking solutions and ethanol dependent states in mice

Abbreviated title: PL activity predicts hedonic value of solutions

Jennifer A. Rinker[1,2,#], Michaela Hoffman[2], Jason Knapp[1], Thomas J. Wukitsch[1], M. Gunes Kutlu[3], Erin S. Calipari[3], Christopher S. McMahan[4], G. Hamilton Baker[5], John J. Woodward[1,2], Patrick J. Mulholland[1,2,#]

[1]Department of Neuroscience, Charleston Alcohol Research Center, Medical University of South Carolina, Charleston SC, 29425

[2]Department of Psychiatry & Behavioral Sciences, Charleston Alcohol Research Center, Medical University of South Carolina, Charleston SC, 29425

[3]Department of Pharmacology, Vanderbilt School of Medicine, Nashville, TN, 37232

[4]School of Mathematical and Statistical Sciences, Clemson-MUSC Artificial Intelligence Hub, Clemson University, Clemson, SC 29634-0975

[5]Department of Pediatrics, Clemson-MUSC Artificial Intelligence Hub, Medical University of South Carolina, Charleston SC, 29425

[#]Corresponding authors: Patrick J. Mulholland mulholl@musc.edu & Jennifer A. Rinker rinker@musc.edu

Conflict of Interest: Authors report no conflict of interest.

Acknowledgements*:* These studies were supported by the Charleston Alcohol Research Center (AA010761), the INIAstress Consortium, and NIH grants AA020930 (PJM), OD021532 (PJM), AA023288 (PJM), and AA025110 (JAR).

Abstract

The medial prefrontal cortex (mPFC) is part of the mesocorticolimbic reward circuitry and integrates information about both salience and valence of stimuli, including drugs and alcohol. While the mPFC has been implicated in regulating aspects of alcohol seeking and consumption, our understanding of how cortical outputs encode motivation to consume is still limited. Here we used fiber photometry to measure calcium activity in putative pyramidal glutamatergic projection neurons in the prelimbic (PrL) mPFC in response to consumption of solutions with varying reinforcing value, i.e., water (nondeprived), ethanol (20% v/v) or sucrose (1% w/v). A similar but distinct pattern of activity emerged across the three solutions during the peri-consummatory phase, such that PrL calcium activity ramped immediately preceding bouts for water, ethanol and sucrose, and scaled with presumed reinforcing value, i.e., water<ethanol<sucrose. Thus, PrL neurons modulate their activity in response to anticipation of drinking bouts, and the population GCaMP6f signal appears to track the hedonic value of different drinking solutions. Further, machine learning of population activity of PrL neurons in anticipation of fluid consumption was sufficient to predict both fluid consumption and distinguish between type of reinforcer consumed. To determine if this signal was indeed encoding valence, we adulterated the ethanol solution with quinine and in non-dependent mice, the calcium signal surrounding drinking bouts was reduced, paralleling the decrease in voluntary quinine-adulterated ethanol drinking. This effect was not present in dependent mice, suggestive of reduced sensitivity to the aversive qualities of quinine or increased sensitivity of reinforcing value of the ethanol solution. Using fiber photometry, we also show that the global population of PrL glutamatergic neurons display sustained GCaMP6f "up-states" that last tens to hundreds of seconds. Drinking bouts frequently occurred during these sustained up-states. Although the PrL→NAcore projection is thought to drive reward-guided behavior, the GCaMP6f signal surrounding ethanol drinking bouts was similar to the signal for water. Overall, our results demonstrate a functional signature in PrL neurons that aligns with the valence of different rewarding solutions compared to home cage water drinking. In summary, these results suggest that PrL neurons encode the hedonic value of rewarding solutions, and population activity in anticipation of ethanol drinking is disrupted by induction of ethanol dependence.

Significance statement

The PrL mPFC has been implicated in mediating aspects of alcohol consumption and seeking, but how and whether the PrL encodes aspects of reward differentially is not clear. Here we show that the PrL shows similar but distinguishable glutamatergic population level calcium activity patterns in response to anticipation of solutions with presumed variance in hedonic value (water, ethanol and sucrose). Contrary to our presumption, PrL→NAcore did not differently encode ethanol drinking compared to water, but ethanol dependence was sufficient to disrupt normal modulation of calcium activity in response to reward devaluation. We present evidence of PrL signatures that track presumed hedonic value, that is disrupted by ethanol dependence.

Introduction

The prefrontal cortex (PFC) regulates executive functioning and goal-directed actions (Buschman and Miller, 2014; Fuster, 2015) and its function can be profoundly impacted by excessive alcohol drinking (Schacht et al., 2013; Mulholland et al., 2016; Blaine et al., 2020; Cannady et al., 2021). Alcohol-induced deficits to PFC function can lead to craving and cognitive dysfunction that interfere with recovery efforts in individuals with alcohol use disorder (AUD; Loeber et al., 2009; Pitel et al., 2009; Stavro et al., 2013). With a lifetime AUD prevalence of upwards of 12% (Hasin et al., 2007) and binge drinking rates up 8% (Grucza et al., 2018), efforts aimed at understanding alcohol's impact on cortical function and how the PFC regulates drinking behaviors is of high importance.

The prelimbic (PrL) cortex is a subregion of the medial aspect of the PFC involved in ethanol seeking behaviors, as well as excessive and compulsive ethanol drinking. Rodent studies have shown that inactivation of the PrL reduces ethanol self-administration in rats (Samson and Chappell, 2001; Palombo et al., 2017), and rats will self-administer ethanol directly into the PrL cortex (Engleman et al., 2020). Chronic exposure to ethanol in rodents produces functional (Kroener et al., 2012; Trantham-Davidson et al., 2014; Pleil et al., 2015b; Klenowski et al., 2016; Varodayan et al., 2018; Hughes et al., 2019; Hughes et al., 2020; Joffe et al., 2020, 2021), molecular (Melendez et al., 2012; Barbier et al., 2017), and morphological (Kroener et al., 2012; Klenowski et al., 2016; Varodayan et al., 2018; Frost et al., 2019; Cannady et al., 2021) neuroadaptations in the PrL cortex. Importantly, these adaptations are proposed as critical drivers of behavioral deficits related to cognitive performance (Kroener et al., 2012; Hu et al., 2015) and compulsive ethanol drinking (Seif et al., 2013; Barbier et al., 2015; Barbier et al., 2017; Barbier et al., 2021).

mPFC neurons can encode anticipatory and goal-directed drinking behaviors (Amiez et al., 2006; Petyko et al., 2009; Horst and Laubach, 2013; Jezzini et al., 2013; Parent et al., 2015; Amarante et al., 2017; Linsenbardt et al., 2019). A recent study revealed that calcium activity in medial PFC glutamatergic projection neurons that innervate the dorsal periaqueductal gray can predict future compulsive drinking (Siciliano et al., 2019). In addition, Linsenbardt and colleagues demonstrated a unique pattern of neural activity in the medial PFC neurons of Wistar rats that encoded the intention to drink alcohol (Linsenbardt et al., 2019). They reported increased firing activity associated with a cue that predicted subsequent ethanol availability and a peak in neural firing post-ethanol drinking. Interestingly, the neural signal encoding the intention to drink alcohol in Wistar rats was blunted in alcohol-preferring P rats. Because of the importance of neural activity in the PrL cortex during active ethanol drinking and adaptations in the PrL produced by chronic ethanol exposure that drive excessive and compulsive ethanol-seeking behaviors, we first sought to determine how ethanol dependence alters population activity of PrL glutamatergic projection neurons during voluntary ethanol drinking. We compared the neural activity patterns surrounding ethanol drinking with the signal for water and sucrose intake. A second focus of this study was to determine how adulterating ethanol with quinine changes the neural activity pattern of PrL

neurons before and after induction of ethanol dependence. To achieve these goals, we used fiber photometry recordings of GCaMP6f calcium transients to define neural activity patterns while mice were actively drinking in their home cages prior to and following chronic intermittent ethanol (CIE) exposure. Because machine learning (ML) can predict neural activity from behavior (Benjamin et al., 2018; Siciliano et al., 2019; Kutlu et al., 2021), we applied two different ML algorithms to determine if the signature of neural activity preceding drinking behavior can predict the solution.

Materials and Methods

Subjects

Male C57BL/6J mice (n = 29) were obtained from Jackson Laboratories (Bar Harbor, ME; strain # 000664) at 7-8 weeks of age. They were group-housed (4/cage) and allowed to acclimatize to the colony room for at least one week in a temperature and humidity-controlled AAALAC-approved facility. Mice were maintained on a reverse 12-h light/dark cycle with lights off at 09:00 am and had ad libitum access to food and water. All animals were treated in strict accordance with the NIH Guide for the Care and Use of Laboratory Animals (National Research Council (U.S.). Committee for the Update of the Guide for the Care and Use of Laboratory Animals. et al., 2011) and all experimental methods were approved by the Medical University of South Carolina's Institutional Animal Care and Use Committee.

Surgery

After acclimation, mice underwent stereotaxic surgery in preparation for fiber photometry recordings. Mice were deeply anesthetized with vaporized isoflurane (1-3%, SomnoSuite Vaporizer, Kent Scientific) and 200 nl of AAV1-CaMKII-GCaMP6f (Addgene, Catalog #100834-AAV1) was microinfused into the PrL cortex (AP: +1.70; ML: ±0.4; DV: -2.35; in mm relative to bregma) at a rate of 100 nL/min. The microinjection needle remained in place for 5 min post-infusion. To target PrL neurons that project to the NAcore, a retrograde AAV-Cre (Addgene, Catalog #107738-AAVrg) was infused into the NAcore (AP: +1.20; ML: ±0.8; DV: -4.60; in mm relative to bregma) and a Cre-dependent GCaMP6f (Addgene, Catalog #100833-AAV1) was infused into the PrL. After AAV infusion, optical ferrules (400 μm, 0.48 NA, 2.5 mm OD ceramic; Doric Lenses) were implanted above the infusion site in one hemisphere and secured via Herculite dental resin (Kerr Dental). Mice were transferred to individual home cages and allowed to recover for 4-6 weeks before initiating fiber photometry recordings. Mice were habituated to handling, tethering to patch cords and lickometer circuitry (MedAssociates) during the recovery period.

Ethanol drinking

After surgery, mice remained on a 12 h light/dark cycle, and food and water were available ad libitum during the experiment except when ethanol or sucrose was presented in their home cages. Binge-like ethanol consumption was induced using a modified 4-d drinking-in-the-dark (DID) protocol (Rhodes et al., 2005; Rhodes et al., 2007; Pleil et al., 2015a; Rinker et al., 2017). Fiber photometry recordings occurred on the 4th day of each cycle of DID, and the drinking sessions lasted for a 2-hr period beginning

3 hr into the dark cycle. In the first cohort of mice (n = 9 mice), standard water bottles were replaced with a single bottle of water for the test drinking sessions in week 1. For test weeks 2 through 4, water was replaced with a single bottle containing 20% ethanol (v/v). After a 2- to 4-wk abstinence period from ethanol drinking, mice were given access to a single bottle containing 1% sucrose (w/v) for the test drinking sessions. In the second cohort (n = 10 mice), mice were allowed to drink ethanol in the DID protocol for 3 weeks prior to and 1 week after exposure to chronic intermittent ethanol in vapor inhalation chambers. Mice in the 3rd cohort (n = 5 mice) were treated in the same manner with the addition of a test drinking session where 250 μM quinine was added to the ethanol solution before and after CIE exposure. An additional cohort of mice (n = 5 mice) that received dual AAV injections in the PrL and NAcore were allowed to drink in the limited-access two-bottle choice model (water vs 15% ethanol, v/v; 2-hour access; (Padula et al., 2015). These mice were given access to two bottles of water for two weeks followed by 3 weeks of access to water and ethanol. Following the conclusion of behavioral experiments, mice were transcardially perfused with Dulbecco's PBS and 4% paraformaldehyde and ferrule placements were histologically verified via the visualization of fiber tracks and viral vector transduction efficiency via GCaMP6f expression.

Chronic Intermittent Ethanol (CIE) vapor exposure

Mice were treated with repeated cycles of ethanol vapor exposure, as previously described (Becker and Lopez, 2004; Lopez and Becker, 2005; Padula et al., 2015). Air or CIE exposure was delivered 16 hr/day for four consecutive days followed by three days of abstinence before beginning the next cycle of ethanol exposure. Before entry into the ethanol chambers for each exposure period, CIE mice received a priming dose of ethanol to initiate intoxication (1.6 g/kg; 8% w/v in sterile saline; 20 ml/kg injection volume; IP) and pyrazole (1 mmol/kg), an alcohol dehydrogenase inhibitor to slow alcohol metabolism. Air-exposed mice were handled similarly but received pyrazole (1 mmol/kg; IP) without ethanol in sterile saline. Ethanol (95%) was volatilized by passing air through a submerged air stone and the resulting vapor was mixed with fresh air and delivered to Plexiglas inhalation chambers (5 L/min) to maintain consistent ethanol concentrations between 17-21 mg/L air in the chamber. Mice were exposed to ethanol vapor at concentrations that yield blood ethanol concentrations (BECs) in the range of 175-225 mg/dL. BECs in samples taken from the retroorbital sinus were determined using an Analox Analyzer (Analox Instruments, Stourbridge, UK), as described previously (Lopez and Becker, 2005). This was repeated each week for 4 consecutive weeks.

In vivo fiber photometry recordings

GCaMP6f transients were recorded in the PrL cortex during 2-hr drinking sessions using fiber photometry. The fiber photometry system consists of 405 and 470 nm light-emitting diodes (LED) coupled into a 400 μm 0.48 NA optical fiber (Doric Lenses) connected to an integrated fluorescent mini-cube containing dichroic mirrors and bandpass filters (Doric Lenses). Excitation power was set to 15 μW for each channel. The optical fiber from the mini-cube connected to a pigtailed rotary joint (FRJ_1x1_PT, Doric Lenses) and

the optic fiber from the rotary joint connected to the implanted fiber using a ceramic sleeve or pinch connector (Thorlabs). The pigtailed rotary joint was suspended in a custom-build balance arm that allowed free movement during the home cage drinking sessions. Emission light was focused onto a photodetector (Newport model 2151; DC low setting) low-passed filtered at 3 Hz and sampled at 6.1 kHz by a RZ5P lock-in digital processor (TDT) controlled by Synapse software (TDT). Excitation light was sinusoidally modulated at 531 Hz (405 nm) and 211 Hz (470 nm) via software control of an LED light driver (Thorlabs). Real-time demodulated emission signals from the two channels were acquired at a frequency of 1017.25 Hz and stored offline for analysis. In the drinking studies, data from lickometers were also collected via TTL inputs to the digital processor. All patchcords were photobleached using a 405 nm LED at 500 μW power for >12 h every 3-4 days to reduce autofluorescence.

Raw photometry data were processed and time-locked to TTLs using custom written functions in MATLAB (Mathworks) software. Because the 405 nm and 470 nm signals showed differences in photobleaching over time (slope measured over single recordings sessions, mean ± SEM; 405 nm -0.056 ± 0.001, 470 nm -0.0042 ± 0.0004, paired t-test, $t_{44} = 2.347$, $p = 0.023$, n = 45 recordings), the signals for each channel were first fitted to a polynomial versus time and then subtracted from one another to calculate the % $\Delta F/F$ time series (Meng et al., 2018). GCaMP6f events were quantified using the 'findpeaks' function in MATLAB (Steinmetz et al., 2017). Events were defined as peaks in the normalized GCaMP6f signal where the median absolute deviation (MAD) was >2 (Gunaydin et al., 2014; Calipari et al., 2016). Next, we determined the peak in the normalized GCaMP6f signal that occurred 3 seconds prior to and after each licking bout. In addition, the minimum GCaMP6f value was determined during each drinking bout to quantify the drop in the signal that occurred during active licking. Finally, the average GCaMP6f signal preceding each licking drinking bout was determined in 10 sec epochs for 1 min. The area under the curve for the GCaMP6f signal was calculated for the 30 second period preceding and following each drinking bout. Based on existing data on the microstructure of rodent drinking behavior (Davis and Smith, 1992; Boughter et al., 2007; Johnson et al., 2010), a licking 'bout' was identified if lick frequency was >4.5 Hz, the interlick interval was < 500 ms, and the bout duration was > 500 ms. In our initial experiments, we observed sustained increases in the GCaMP6f signal that were reminiscent of persistent cortical up-states (Seamans et al., 2003), but lasted tens to hundreds of seconds. Prolonged GCaMP6f up-states were defined as increases in the signal above one median absolute deviation that lasted >1 second. Slope and intercept variables for the 30 seconds preceding each drinking bout were derived from a linear mixed-effects model ("lme4" package; Bates et al., 2015) and optimized using the "nlminb" method ("optimx" package; Nash and Varadhan, 2011) in R.

Machine Learning

A machine learning classifier support vector machine (SVM; Kutlu et al., 2021) was used to determine if the GCaMP6f signal 30 seconds prior to a drinking bout could predict consumption of water, ethanol, or sucrose. A custom MATLAB code was used to create randomly selected training and test data sets for

SVM analysis using the best predictive features in a kernel function (radial basis function, RBF) to find the optimal hyperplane between binary prediction options (Kutlu et al., 2021). Then, the trained model was used to predict the accuracy of classifying the test data set across 20 trials. For SVM analysis, we first compared pre-bout data for each drinking solution with random 30-second epochs using the same number of random epochs as drinking bouts within each recording. Next, we analyzed whether four features of the 30 second pre-bout data (slope, intercept, peak 3 seconds prior to a bout, and AUC) predicted drinking for water, ethanol, or sucrose. Data for the features were log2-transformed, with the exception of slope given the presence of negative values for some water drinking bouts. All data sets were also analyzed using randomly scrambled group classifications.

For multi-class classification, an extreme gradient boosting algorithm (i.e., XGBoost; R package version 0.4-2 1.4 (2015): 1-4.) was selected because of its ability to work with small, sparse data sets and more accurately predict neural data compared with other approaches, included neural networks and generalized linear models (Chen and Guestrin, 2016; Benjamin et al., 2018). XGBoost also allowed us to determine when important features occurred in the pre-bout data while also comparing across all three solutions and random epochs. We first reduced the dimension of the feature space via functional data analysis techniques as was outlined in (Rossi et al., 2005) by viewing the 30 second GCaMP6f signal as data that is arising from an unknown function. Next, an estimator of this function was developed via a B-spline approximation using 300 basis functions. The coefficients from these approximations are then used as the feature set, which reduces the feature space from >30,000 variables to 300, while preserving virtually all of the information available in the 30 second GCaMP6f signal. Custom R code was used to create randomly selected training and test data sets for the XGBoost analysis. Model training made use of repeated 10-fold cross validation, repeated 10 times, to tune the number of regression trees and tree depth of the XGBoost model. To evaluate prediction accuracy, the trained model was used to predict the accuracy of classifying the test data which consisted of 20 trials. This entire process was repeated 100 times. Variable importance was assessed in the usual manner via VIP scores for each of the 100 trained models. To aggregate the VIP scores across the 100 models fits, we computed the average VIP score for each feature and then normalize these scores to exist between 0 and 1 by dividing by the max. The relative importance of the top 20 features were reported.

Histology

GCaMP6f and mCherry expression and chronic optical ferrules location were identified using standard fluorescent histological techniques. Briefly, mice were perfused as described above, and tissue sliced at 40μm on a vibratome (Leica VT 1000S, Leica Biosystems). Images were acquired using a Zeiss LSM 880 confocal microscope.

Statistics

All behavioral and photometry data were analyzed as a general linear mixed model (SAS PROC MIXED; version 9.4) using Tukey post-hoc tests, when applicable, following our previous methods (McGuier et al., 2015; Mulholland et al., 2018). This statistical approach was selected because of its capacity to analyze unbalanced and complex repeated-measures data and the ability to model the variance and correlation structure of repeated-measures experimental designs (Littell et al., 1998). For all repeated measures designs, data were nested within mouse and time. Data are reported as mean ± SEM, and statistical significance was established with $\alpha = 0.05$.

Code Accessibility

All custom written code in MATLAB and R language used for analyses in this manuscript is available upon request.

Results

Voluntary drinking

Mice were allowed to drink water, 20% ethanol, or 1% sucrose in their home cages in a single-bottle limited-access model. We time locked licking behavior for each solution while recording GCaMP6f activity in glutamatergic neurons the prelimbic (PrL) cortex. Mice consumed more sucrose (in ml/kg) than water and ethanol ($F_{2,14} = 4.52$, $p = 0.031$; n = 9 mice; **Fig 1A**). There were significant differences in bout duration (**Fig 1B**) and frequency of licking behavior (**Fig 1C**) for the three solutions (*Duration*: $F_{2,13} = 39.45$, $p < 0.0001$; *Frequency*: $F_{2,13} = 5.99$, $p = 0.014$). Posthoc comparisons showed that lick frequency for ethanol was slower than that for water or sucrose (**Fig 1C**), but bout duration was longer for ethanol than sucrose and water (**Fig 1B**), and bout duration for sucrose was longer than water (**Fig 1B**).

Prelimbic GCaMP6f signaling surrounding drinking bouts

Representative traces of the GCaMP6f signal and licking bouts for water (blue), ethanol (red), and sucrose (gold) drinking sessions are shown in **Fig 1E**. Consistent with evidence of increased neural activity during goal-directed behaviors (Steinmetz et al., 2019), we observed an increase in the PrL GCaMP6f population signal preceding drinking bouts (**Fig 1F**). When analyzing the averaged signal in 10-sec epochs for a 1-min period before each bout, there was a significant main effect of time ($F_{5,45} = 15.40$, $p < 0.0001$) and drinking solution ($F_{2,13}$ 41.00, $p < 0.0001$). The signal in the 10-sec epoch preceding a bout was significantly higher than the other epochs ($p < 0.01$; **Fig 1G**). The 20-11 and 30-21 second epochs were significantly higher than the epochs between 60 and 41 seconds ($p < 0.05$). Posthoc comparisons also revealed that the GCaMP6f signal for sucrose was significantly higher than ethanol and water ($p < 0.0001$), and the signal for ethanol was significantly higher than water ($p = 0.013$). Although the signal preceding water drinking bouts was not as dynamic as ethanol or sucrose, $\Delta F/F$ values were elevated to 1-2% across the 1 min preceding water consumption, suggesting that PrL neurons may also encode the intent to drink water even under non-deprived conditions.

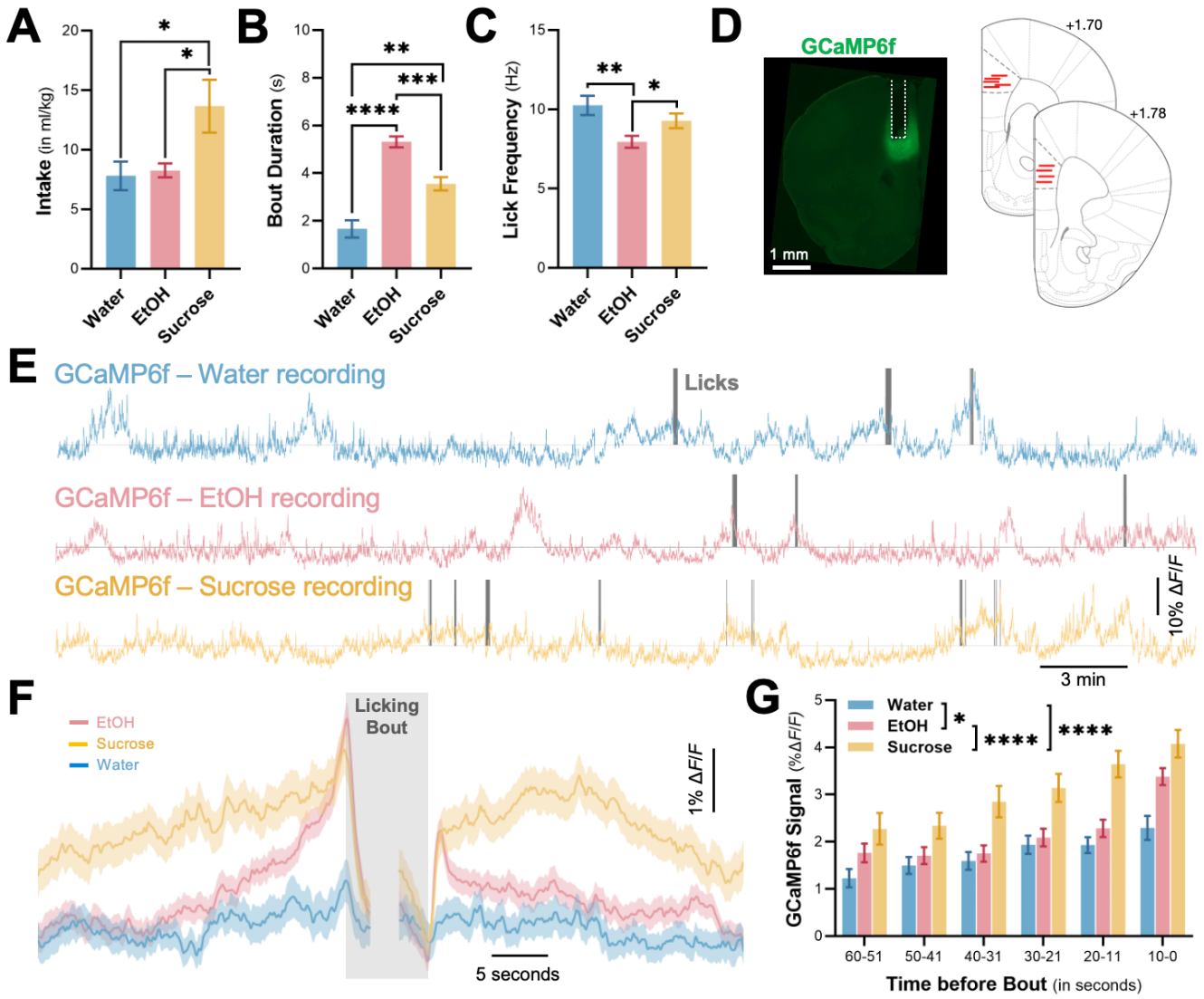

Figure 1. PrL cortex GCaMP6f signaling during water, ethanol (EtOH), and sucrose drinking. ***A-C***, Intake, bout duration, and lick frequency for water, ethanol (20%, v/v), and sucrose (1%, w/v) drinking solutions. ***D***, Representative image of GCaMP6f expression in PrL cortex and location of the chronic optical ferrule implant. ***E***, Representative recordings of normalized GCaMP6f during drinking sessions for water, EtOH, and sucrose. Licks on the sipper tube are demarked by gray vertical lines. ***F***, Averaged GCaMP6f signal prior to and following licking bouts for the three drinking solutions. Averaged traces show mean (solid line) with standard error of the mean (shading). ***G***, Binned GCaMP6f signal preceding licking bouts. *$p < 0.05$; **$p < 0.01$; ***$p < 0.001$; ****$p < 0.0001$.

These results suggest that the GCaMP6f signal, particularly within 30 seconds of the start of drinking bouts, may distinctly encode the anticipation of or decision to consume the three different solutions, which scales with presumed valence of the solution. To first test this, we used a SVM classifier to determine whether the GCaMP6f signal could predict drinking for the individual solutions. The SVM was able to predict when mice were drinking water (74% accuracy; $t_{99} = 17.70$, $p < 0.0001$), ethanol (77.7% accuracy; $t_{99} = 19.22$, $p < 0.0001$), and sucrose (70.8% accuracy; $t_{99} = 16.00$, $p < 0.0001$) compared with random epochs extracted from their respective drinking sessions (**Fig 2B**). We then wanted to determine if the GCaMP6f signal in the 30 seconds preceding drinking bouts was distinct enough across solutions to predict when mice were drinking water, ethanol, or sucrose. The SVM was able to predict whether

mice were drinking ethanol versus water (65.5% accuracy; $t_{99} = 16.01$, $p < 0.0001$), sucrose versus water (64.7% accuracy; $t_{99} = 10.53$, $p < 0.0001$), and ethanol versus sucrose (64.1% accuracy; $t_{99} = 10.88$, $p < 0.0001$). Prediction accuracy for all solutions was significantly different than scrambled classification for within solution and across solution analyses ($t_{198} > 7.148$, $p < 0.0001$). Next, we asked if a separate ML analysis could distinguish between the 30 seconds of pre-bout data for three solutions and random epochs when analyzed together. An extreme gradient boosting classifier (i.e., XGBoost) identified 20 factors of high importance in the 30 seconds of data preceding a drinking bout (**Fig 2C**). A variable importance plot shows that the majority of these factors reside within 10 seconds prior to initiation of licking behavior, and the factors with the highest importance reside within ~5 seconds of bout initiation (**Fig 2C**). XGBoost analysis demonstrated modest, but highly significant accuracy (i.e., 62.4%) for predicting the three drinking solution and random data from one another ($t_{198} = 14.83$, $p < 0.0001$; **Fig 2D**).

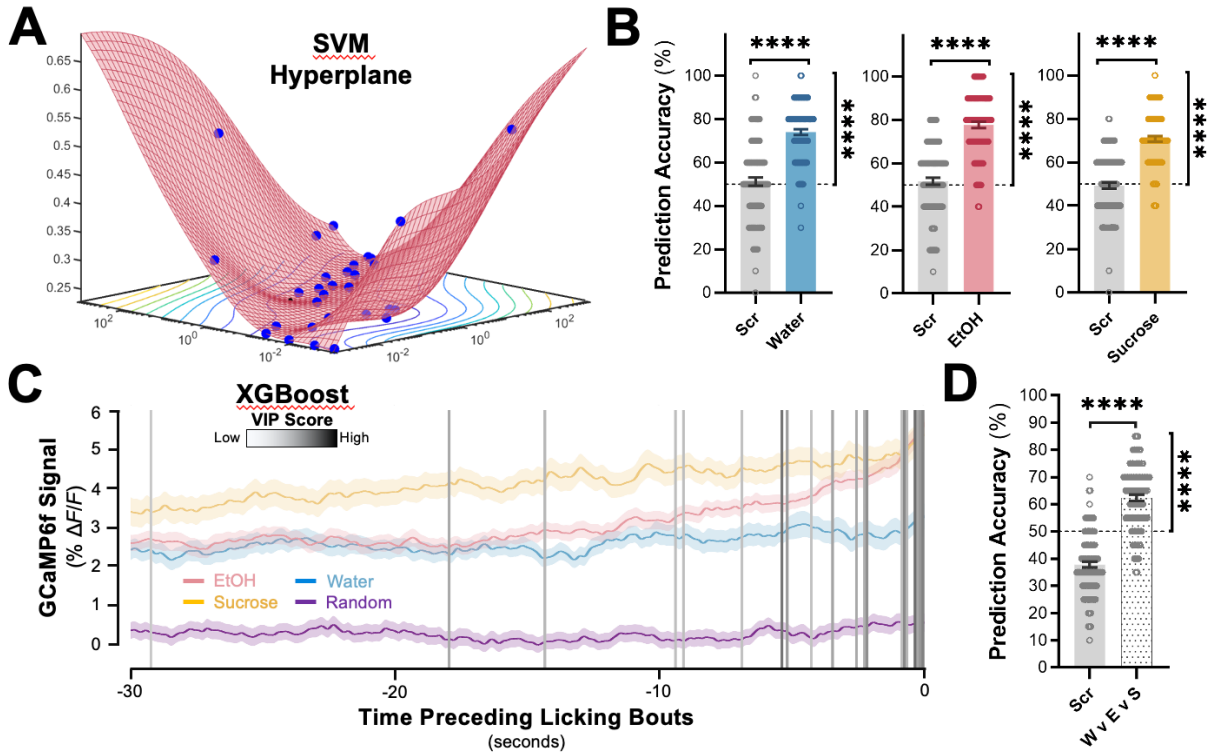

Figure 2. Prediction of different drinking solutions using machine learning approaches. ***A***, Representative support vector machine (SVM) hyperplane for the EtOH vs. random comparison. ***B***, Prediction accuracy for the three different solutions vs. random condition. Accuracy for scrambled (Scr) comparison is also shown. ***C***, Variable importance plot (VIP) locations from the XGBoost algorithm. ***D***, Prediction accuracy for the three different solutions and the random condition. ****$p < 0.0001$.

Because the machine learning analyses suggest that the pre-bout signal encodes some aspect of presumed hedonic value of the different solutions, we next performed a detailed analysis of the GCaMP6f signal surrounding drinking bouts. Analysis of the GCaMP6f signal before, during, and after drinking bouts revealed a significant drinking solution by time interaction ($F_{4,26} = 5.69$, $p = 0.002$; **Fig 3A**). For water only bouts, posthoc comparisons showed that the signal during the bout was significantly lower than the signal

before and after the bout ($p < 0.01$). For ethanol and sucrose bouts, the signal was significantly different at each time point (before > after > during; $p < 0.05$). Posthoc comparison across solutions showed that the signal before an ethanol or sucrose bout was significantly increased compared with the signal before a water bout ($p < 0.0001$). The same was true when comparing the signal after the drinking bouts ($p < 0.01$). In contrast, the signal during a bout was similar across the three solutions ($p > 0.27$). When considering the area under the curve (AUC) of the signal 30 seconds prior to and after a licking bout, there was a significant difference across the 3 solutions ($F_{2,13} = 27.50$, $p < 0.0001$, **Fig 3B**). Post-hoc analyses revealed that the AUC for ethanol was higher than water ($p = 0.034$) and the AUC for sucrose was higher than both ethanol and water ($p < 0.0001$). Because reward signaling for sucrose drinking tracks with satiation (Gunaydin et al., 2014), we compared the peak GCaMP6f preceding the first and last licking bout that occurred within each drinking session across all three solutions. There was a significant main effect of bout ($F_{1,9} = 12.22$, $p = 0.007$), but not a main effect of solution ($F_{2,11} = 1.97$, $p = 0.18$) or a significant interaction ($F_{2,11} = 1.16$, $p = 0.35$). Consistent with previous evidence, the peak preceding the first bout was larger than the peak for the last bout (**Fig 3C**).

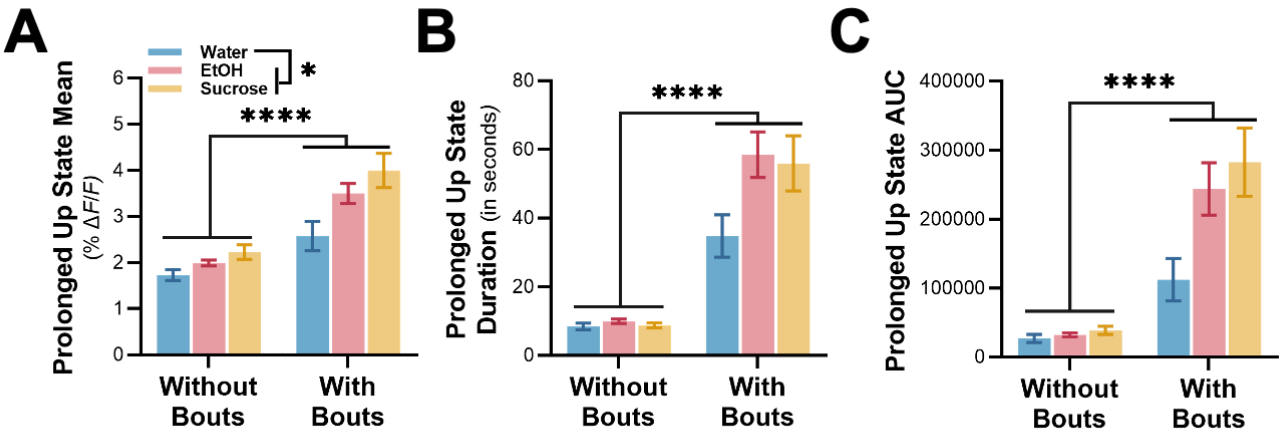

Figure 3. Features of the GCaMP6f signal surrounding licking bouts for the different drinking solutions. ***A***, Peak in the GCaMP6f signal 3 sec before and after licking bouts, and the minimum signal during drinking. ***B***, Area under the curve (AUC) before and after licking bouts. ***C***, Comparison of the peak signal preceding the first and last drinking bout for each solution. *$p < 0.05$; **$p < 0.01$; ****$p < 0.0001$.

Next, we determined if ethanol or sucrose drinking altered GCaMP6f 'events' in the PrL cortex (**Fig 4A**). The frequency ($F_{2,16} = 0.63$, $p = 0.54$), amplitude ($F_{2,16} = 1.56$, $p = 0.24$), and width ($F_{2,16} = 0.70$, $p = 0.51$) of GCaMP6f events during ethanol and sucrose drinking sessions were not significantly different from water drinking sessions (**Fig 4C-E**).

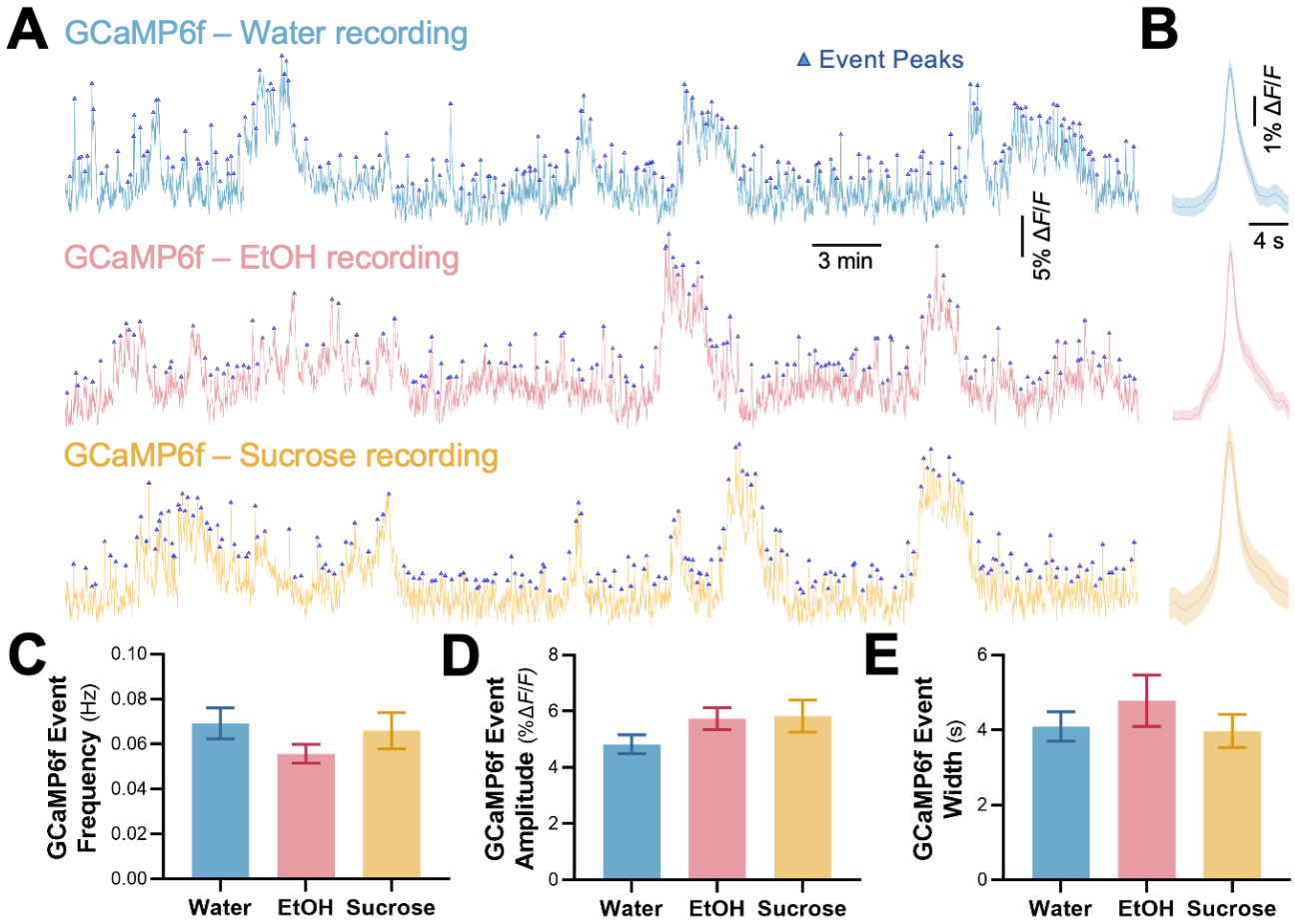

Figure 4. GCaMP6f events are similar across drinking solutions. ***A-B***, Representative traces showing GCaMP6f events and averaged events for water, EtOH, and sucrose. Averaged events show mean (solid line) with standard error of the mean (shading). ***C-E***, GCaMP6f event frequency, amplitude, and width were similar.

Prolonged GCaMP6f up-states and licking behaviors

As suggested by the representative traces shown in **Fig 1A**, licking bouts for water, sucrose, and ethanol appeared to occur during prolonged up-states in the GCaMP6f signal, although not every prolonged up-state contained a licking bout. For the water drinking session, 65.2% of the licking bouts occurred when the GCaMP6f signal was above the threshold (>1 sec and >1 MAD) to meet criteria for a prolonged up-state. This value increased to 80.8% and 90.6% for licking bouts during the ethanol and sucrose drinking sessions, respectively. We then compared the mean GCaMP6f signal, duration, and AUC of prolonged up-states that did and did not contain licking bouts. For each of these measures, there was a significant main effect revealing increases when bouts were present (*mean*: $F_{1,9} = 58.5$, $p < 0.0001$; *duration*: $F_{1,9} = 74.88$ $p < 0.0001$; *AUC*, $F_{1,9} = 45.07$, $p < 0.0001$; **Fig 5A-C**). There was also a significant main effect of solution ($F_{2,17} = 7.47$, $p = 0.005$) for the mean of the GCaMP6f signal during prolonged up-states, with posthoc analyses indicating that the up-state mean for ethanol and sucrose were higher than water ($p < 0.05$).

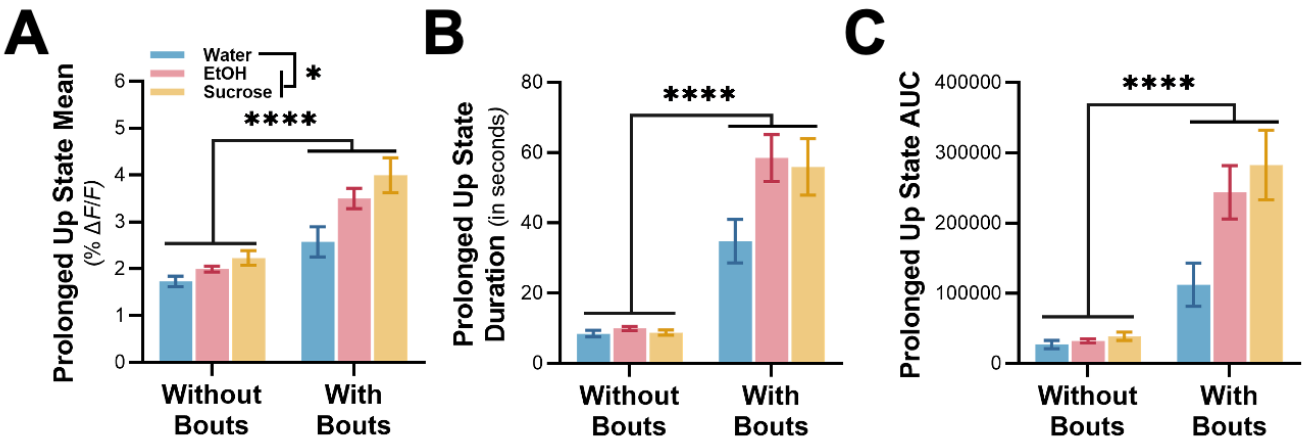

Figure 5. Features of prolonged GCaMP6f up-state differed with and without drinking bouts. ***A-C***, Mean, duration, and AUC of prolonged up-states were greater when it contained a licking bout. Prolonged up-state mean was also greater for EtOH and sucrose vs. water. *$p < 0.05$; ****$p < 0.0001$.

Prelimbic-to-accumbens circuitry and two-bottle choice drinking

PrL glutamatergic projections to the nucleus accumbens core (NAcore) are important for regulating goal-directed behaviors and for seeking abused drugs over natural rewards (Peters et al., 2009; Moorman et al., 2015; Nall et al., 2021). To determine if there are differences in calcium signaling in PrL→NAcore projection neurons for ethanol and water consumption, we injected Cre-expressing retrograde AAV into the NAcore and a Cre-dependent AAV expressing GCaMP6f in the PrL and implanted an optical ferrule in the PrL above the infusion site. To compare the GCaMP6f transients surrounding licking bouts for water and ethanol simultaneously, these mice were allowed to drink in a two-bottle choice, limited-access model. During a baseline period of water availability in both bottles, there was a peak in the GCaMP6f signal prior to and after licking bouts with a marked drop in the signal during licking (**Fig 6G**; n = 5 mice). When given the choice between ethanol and water, mice consumed ~1.9 g/kg of ethanol in 2 h and had an 86% preference for ethanol over water (**Fig 6E**). Similar to the data shown in **Fig 1B**, bout duration was significantly longer for ethanol compared with water ($F_{1,3} = 10.32$, $p = 0.0489$; **Fig 6D**). Contrary to our hypothesis that the PrL→NAcore would encode for ethanol over water, the GCaMP6f signal surrounding licking bouts for ethanol were similar to those for water (main effect of solution: $F_{1,3} = 3.99$, $p = 0.14$; **Fig 6H**). The AUC measurement of the GCaMP6f signal surrounding ethanol drinking bouts was significantly smaller than the AUC for the water signal ($F_{1,3} = 10.72$, $p = 0.047$, **Fig 6I**).

In these mice, 55% of the licking bouts for water occurred when the GCaMP6f signal in PrL→NAcore projection neurons surpassed the criteria for a prolonged up-state. When mice licked for ethanol, only 45.2% of the bouts occurred during an up-state. Unlike the recordings from all PrL projection neurons, the mean GCaMP6f signal during prolonged up-states did not differ between ethanol and water licking bouts ($F_{1,4} = 1.04$, $p = 0.365$, **Fig 6J**) or when an up-state contained a drinking bout ($F_{1,4} = 1.31$, $p = 0.316$). Because of the similarity in the GCaMP6f signal metrics when mice were drinking water and ethanol in

PrL→NAcore projections, the remainder of the studies analyzed the population GCaMP6f signal in all glutamatergic PrL projection neurons.

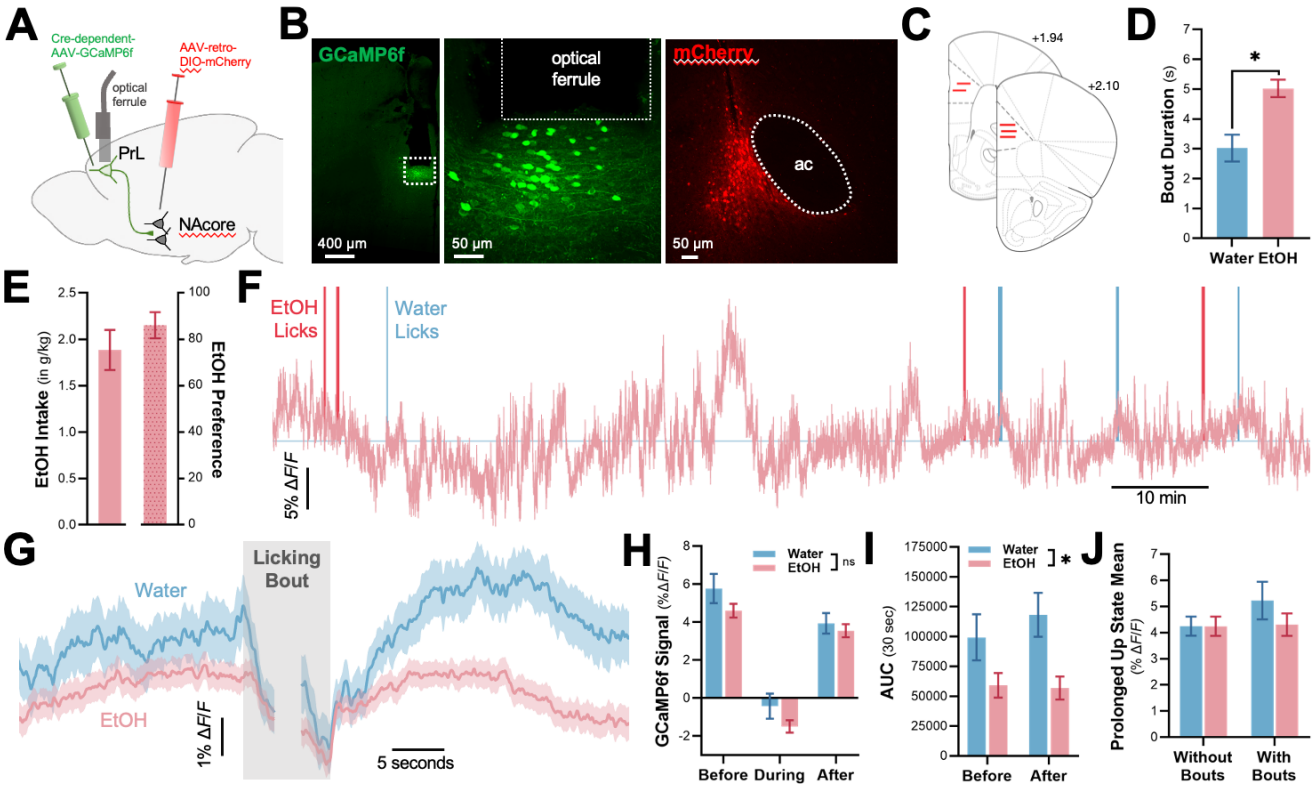

Figure 6. Encoding of water and EtOH in PrL→NAcore projection neurons. ***A***, Schematic of viral approach to record from PrL neurons that project to the NAcore. ***B***, Representative image of GCaMP6f in mCherry+ PrL→NAcore projection neurons. ***C***, Schematic of location of the chronic optical ferrule implants. ***D***, Bout duration for water and EtOH in a two-bottle, limited-access choice model. ***E***, EtOH intake and preference. ***F***, Representative normalized GCaMP6f signal and licks for water or EtOH. ***G***, Averaged GCaMP6f signal for water and EtOH surrounding licking bouts. ***H***, Quantified GCaMP6f signal before, during, and after licking bouts for water vs. EtOH. ***I***, AUC before and after licking bouts. ***J***, Prolonged up-state mean with and without drinking bouts for water and EtOH. *$p < 0.05$.

CIE exposure and prelimbic GCaMP6f signaling

Now that we distinct calcium signaling in the PrL cortex of mice drinking in the DID model, we next wanted to determine how the induction of ethanol dependence alters the GCaMP6f signal surrounding drinking bouts. Mice consumed ethanol in their home cages for 3 weeks during photometry recordings and were then pseudo-randomly assigned to either air or ethanol exposure in vapor inhalation chambers based on their baseline ethanol intake. While ethanol drinking was similar during baseline, CIE exposure increased drinking (in g/kg) in ethanol dependent mice during the post-vapor test drinking sessions (treatment x time interaction: $F_{1,8} = 19.12$, $p = 0.002$; n = 5 mice/group; **Fig 7A**). There was also a significant interaction for bout duration ($F_{1,8} = 14.62$, $p = 0.005$), where CIE exposure increased the duration of ethanol drinking bouts (*Pre-CIE*: 3.81 ± 0.31; *Post-CIE*: 6.33 ± 0.47, $p = 0.003$). Bout duration in air controls ($p = 0.14$) and lick frequency in both treatment groups ($F_{1,8} = 1.82$, $p = 0.215$) were similar.

Consistent with recordings in the first experiment, there were peaks in the GCaMP6f signal prior to and after drinking bouts for ethanol prior to vapor chamber exposure (**Fig 7B**). The GCaMP6f signal surrounding licking bouts pre- and post-Air or -CIE vapor exposure was analyzed by a repeated-measures 3-way mixed linear model. There was a significant time (pre- and post-vapor) x treatment (air vs CIE) x signal (before, during, after licking) 3-way interaction ($F_{2,575} = 3.06$, $p = 0.047$, n = 5 mice/group). Analyses of simple interactions before, during, and after licking bouts revealed a significant interaction between treatment and time for the signal before ($F_{1,607} = 7.45$, $p = 0.007$), but during ($F_{1,607} = 0.14$, $p = 0.713$) or after ($F_{1,607} = 3.19$, $p = 0.075$) drinking bouts. The simple analysis of the GCaMP6f signal prior to licking bouts demonstrated that the signal significantly decreased ($p = 0.0005$) in the air exposed controls from the pre-air vapor exposure. However, the signal in the CIE exposed mice did not change compared to their pre-vapor baseline values ($p = 0.901$). For the GCaMP6f signal during drinking bouts, there was a significant main effect of time ($F_{1,607} = 9.92$, $p = 0.002$), but not treatment ($F_{1,607} = 0.03$, $p = 0.868$). The post-vapor exposure signal during the bout in both groups was significantly lower than the baseline values. There were also main effects of time ($F_{1,607} = 12.05$, $p = 0.0006$) and treatment ($F_{1,607} = 9.72$, $p = 0.0019$) for the GCaMP6f signal that occurred after a drinking bout showing a reduction in the amplitude compared with the pre-vapor exposure values and the CIE-exposed mice, respectively. To best represent the signal changes surrounding licking bouts after air or ethanol vapor exposure, **Fig 7E** shows the raw change in the GCaMP6f signal (post-vapor minus baseline) in the two treatment groups. Closer inspection of the GCaMP6f signal preceding and during a drinking bout in **Fig 7C** suggested that the signal change was greater in the CIE exposed mice. To test this directly, we calculate the difference in the raw GCaMP6f signal before and during licking bouts. In a two-way, repeated measures analysis, there was a significant interaction between time and treatment ($F_{1,8} = 7.67$, $p = 0.024$). Post-hoc analyses indicated that difference in the GCaMP6f signal between these two time points was significantly greater in the CIE exposed mice ($p = 0.039$, **Fig 7F**), but not the air vapor exposed controls ($p = 0.142$).

Next, we determined if there were other measures of the GCaMP6f signal that were affected by treatment or time. CIE exposure did not affect GCaMP6f event amplitude ($F_{1,8} = 1.84$, $p = 0.212$), width ($F_{1,8} = 1.93$, $p = 0.202$), or frequency ($F_{1,8} = 0.98$, $p = 0.351$) compared with Air controls. However, there was a main effect for time that revealed a significant reduction in the amplitude ($F_{1,8} = 12.80$, $p = 0.007$) and width ($F_{1,8} = 12.13$, $p = 0.008$) of GCaMP6f events with a concomitant increase in GCaMP6f event frequency when comparing pre- and post-vapor chamber exposure ($F_{1,8} = 10.37$, $p = 0.012$). The effects related to time could be due to degradation or instability of the GCaMP6f signal. As a quantitative measure of the stability of the GCaMP6f signal across time, we calculated the mean fluorescent signal of the raw 405 and 470 nm signals. The analysis showed that the average raw values for the two channels were similar pre- and post-vapor exposure (*405 nm*: $F_{1,8} = 0.21$, $p = 0.660$; *470 nm*: $F_{1,8} = 0.04$, $p = 0.838$) and were not affected by CIE (*405 nm*: $F_{1,8} = 0.08$, $p = 0.786$; *470 nm*: $F_{1,8} = 0.16$, $p = 0.700$).

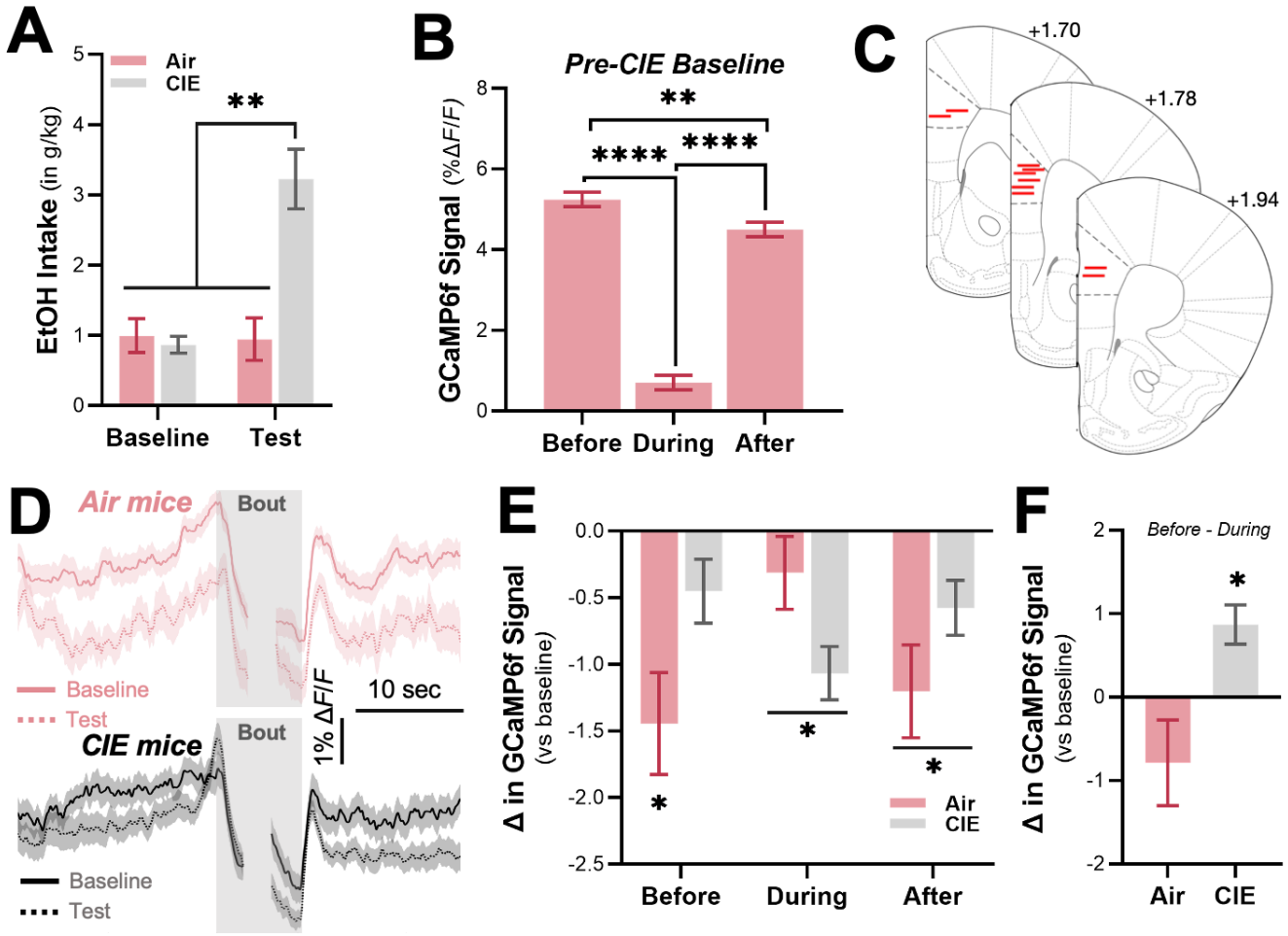

Figure 7. Effects of CIE on PrL GCaMP6f activity. ***A***, EtOH intake in Air and CIE exposed mice at baseline and during the post-CIE test. ***B***, Quantified GCaMP6f signal before, during, and after bouts of licking for EtOH prior to CIE exposure. ***C***, Schematic of location of the chronic optical ferrule implants. ***D***, Averaged GCaMP6f signal surrounding licking bouts for EtOH in Air (red) and CIE (gray) before and after CIE (or Air) exposure. ***E***, Change in GCaMP6f signal from baseline. ***F***, Difference from peak before to min during bouts of licking for EtOH. *$p < 0.05$, **$p < 0.01$, ****$p < 0.0001$.

Quinine-resistant drinking and prelimbic GCaMP6f signaling

Because the medial PFC controls excessive and compulsive-like ethanol drinking (Pfarr et al., 2015; Siciliano et al., 2019), we next determined how quinine adulteration of ethanol affected the PrL GCaMP6f signal in ethanol dependent mice. Prior to CIE exposure, the addition of 250 μM quinine to the ethanol drinking solution significantly reduced intake in mice (interaction: $F_{1,4} = 8.03$, $p = 0.047$; post-hoc, $p = 0.009$; n = 5 mice; **Fig. 8A**). The GCaMP6f signal surrounding licking bouts for ethanol and quinine-adulterated ethanol pre- and post-CIE exposure were analyzed using a within-subjects, three-way mixed linear model. The 3-way interaction was not significant ($F_{2,713} = 0.50$, $p = 0.609$), but there was a significant treatment x drinking solution interaction ($F_{1,713} = 10.63$, $p = 0.001$). Post-hoc analysis from the simple effects analysis demonstrated that the GCaMP6f signal was significantly reduced when mice consumed ethanol adulterated with quinine during the pre-CIE drinking test ($p = 0.009$, **Fig 8C**). In contrast, these

mice consumed equal amounts of ethanol when quinine was added to the drinking solution during the post-CIE test (posthoc, p = 0.531; **Fig 8A**), and the GCaMP6f signal surrounding drinking bouts was unaltered (p = 0.748, **Fig 8C**). The SVM predicted the quinine-induced change in the calcium signal prior to, but not after CIE exposure (t_{198} = 11.59, p < 0.0001; **Fig 8D**).

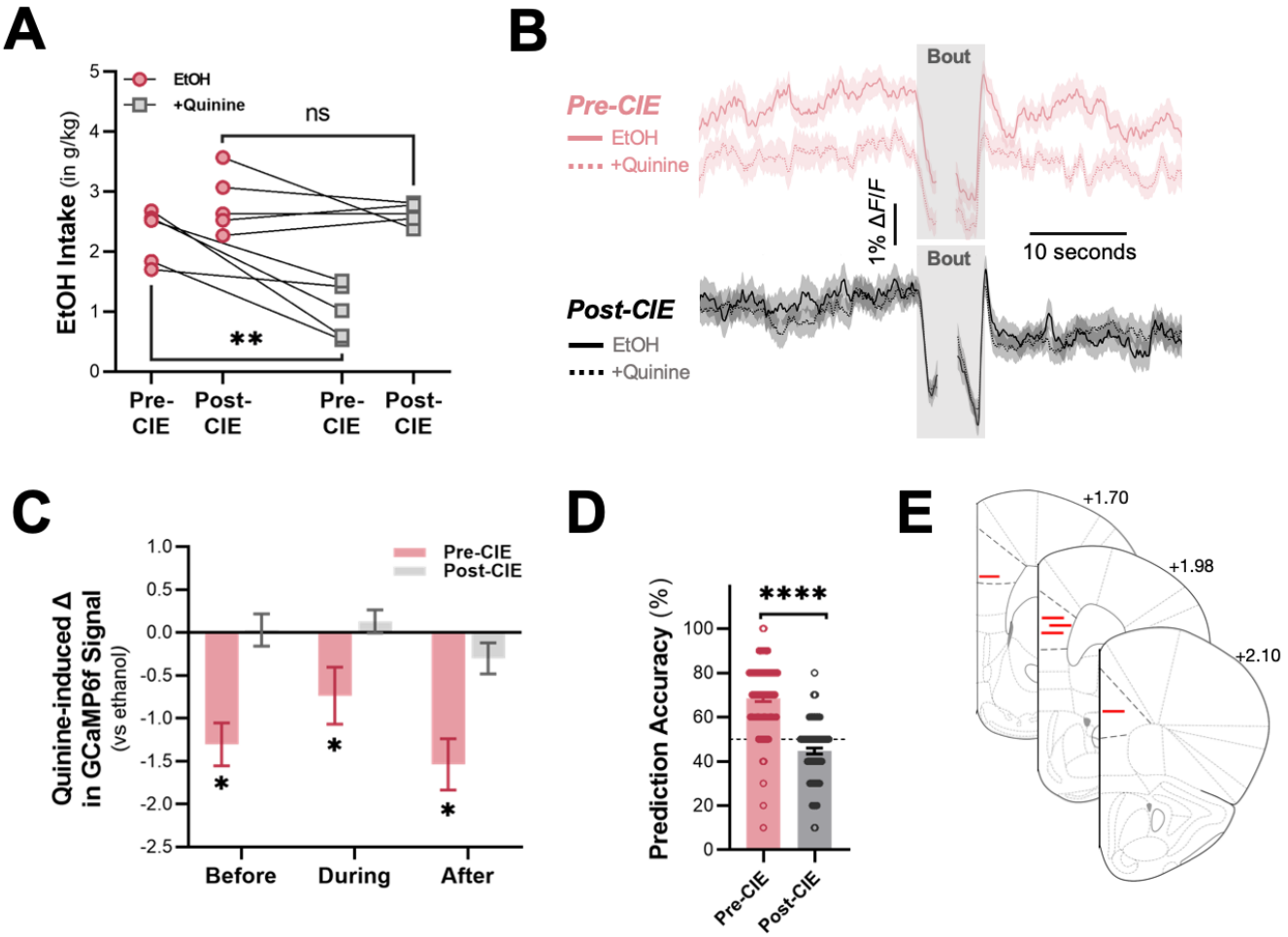

Figure 8. EtOH dependence blocks quinine-induced PrL GCaMP6f signal reduction. ***A***, EtOH intake pre-CIE and post-CIE (red), and during quinine-adulteration test (gray). ***B***, Averaged GCaMP6f signal for EtOH and quinine-adulterated EtOH bouts pre- and post-CIE. ***C***, Quinine-induced change in GCaMP6f signal before, during, and after licking bouts pre- and post-CIE. ***D***, SVM prediction accuracy for distinguishing EtOH bouts from EtOH+quinine bouts pre- and post-CIE. ***E***, Schematic of location of the chronic optical ferrule implants. *$p < 0.05$, **$p < 0.01$, ****$p < 0.0001$.

Discussion

In this study, we provide experimental and computational evidence from a supervised machine learning model that PrL pyramidal population activity patterns track the perceived hedonic value of rewarding solutions in male C57BL/6J mice voluntarily drinking in a home cage model. One striking finding from these studies is that ramping of PrL activity predicts drinking behavior for three solutions with differing hedonic value. Moreover, we showed that mice predominantly consumed fluid when the PrL population signal was in a prolonged upstate, and features of the pre-bout ramping signal could accurately discriminate between the three drinking solutions. Consistent with a declining VTA signaling for sucrose

licking within a single drinking session reflecting satiety-induced reductions in reinforcing value (Gunaydin et al., 2014), we observed a decrease in the peak calcium signal for all solutions across time. Another main finding from our study is that the pre-bout PrL signal parallels escalated and compulsive drinking behavior in a mouse model for the study of AUD, i.e., remains elevated in dependent animals that show aversion-resistant (quinine adulteration) consumption of ethanol, but is diminished in control animals sensitive to quinine adulteration. Overall, our results provide evidence for a functional signature in the PrL cortex that aligns with the salience of reward-related behaviors likely signaling the intention to drink, even when mice are rendered dependent upon ethanol.

Anticipatory PrL signaling and licking behavior

Our data extend previous findings by providing evidence for anticipatory reward signaling in the population of PrL glutamatergic projection neurons in non-deprived mice freely moving in their home cage. The population calcium signal was elevated prior to drinking bouts and peaked just prior to licking bouts for ethanol or sucrose. We also observed ramping of calcium activity in PrL→NAcore projection neurons prior to water and ethanol drinking bouts in a two-bottle choice model. The ramping of the cortical GCaMP6f signal prior goal-directed behavior is consistent with single unit data (Narayanan and Laubach, 2009; Ma et al., 2014; Emmons et al., 2017; Steinmetz et al., 2019), although our photometry data showed longer ramping time-scales preceding consumption, perhaps reflecting anticipatory signaling at the population level. In addition, we also observed 'prolonged' up-states in the GCaMP6f signal over the course of the drinking sessions that last quite longer (>60 seconds) than traditionally defined 'persistent' cortical up-states (Seamans et al., 2003). Interestingly, drinking bouts frequently occurred during these prolonged up-states, and characteristics of the prolonged up-states in the PrL population were quantitatively different in the presence of a drinking bout, especially for ethanol and sucrose. While the prolonged up-states appear important for signaling drinking, some prolonged up-states occur in the absence of drinking, suggesting that additional signaling outside of the PrL or within a specific PrL projection is necessary. Together, these data suggest that population calcium activity in PrL glutamatergic neurons and those that projection to the NAcore encode the intent to drink rewarding (i.e., ethanol, sucrose) and necessary (i.e., water) solutions.

PrL neurons encode hedonic value

Consistent with evidence that single unit activity in the medial PFC encodes the magnitude of the reward (Amiez et al., 2006; Jezzini et al., 2013; Amarante et al., 2017), the anticipatory photometry signal preceding drinking bouts appeared to track the perceived hedonic value of each solution tested in this study. We found that multiple features of the pre-bout GCaMP6f signal that differed across the three drinking solutions. Specifically, there were differences in the pre-bout ramping, as well as the AUC and peak in the signal before and after licking bouts. Whereas peaks for ethanol and sucrose were similarly increased above peaks surrounding water bouts, the other measures showed differences across all three

solutions. Presumably, ethanol is more rewarding than water, reflected by the longer duration of ethanol licking bouts under non-water deprived conditions, and these same mice consumed more sucrose (in ml/kg) than ethanol and water. To further support evidence for encoding of hedonic value by PrL neurons prior to goal-directed behaviors, machine learning analyses predicted drinking bouts against both random epochs of the calcium signal and when mice were drinking each of the three solutions. In addition to these computational findings, pairing ethanol with the aversive, bitter tastant quinine in non-dependent mice not only produced the expected reduction in ethanol consumption, but also reduced the GCaMP6f signal surrounding drinking bouts. Finally, the peak GCaMP6f signal preceding drinking decline within individual drinking sessions for all solutions, which may explain the modest, but highly significant differences identified by the ML analyses. Thus, these studies provide multiple lines of evidence that population activity of PrL projection neurons encodes the hedonic value of different drinking solutions.

CIE exposure and anticipatory PrL signaling

Previously, calcium activity in dorsal periaqueductal gray-projecting PrL neurons predicted future compulsive ethanol drinking (Siciliano et al., 2019). While we did not design our study to predict subsequent drinking phenotypes, we measured population activity of PrL neurons following CIE exposure when mice display a compulsive-like phenotype (Lopez et al., 2014; Radke et al., 2017; Renteria et al., 2020; Gioia and Woodward, 2021). In the air control mice, the GCaMP6f signal surrounding ethanol drinking bouts decreased across time, which is consistent with previous evidence of signal habituation to repeated reward access (Gunaydin et al., 2014). Whereas quinine adulteration reduce drinking and the calcium signal in control mice, the addition of quinine did not affect drinking in CIE-exposed mice, and the calcium signal surrounding drinking bouts remained elevated, possibly reflecting known PrL adaptations produced by CIE exposure (Kroener et al., 2012; Pleil et al., 2015b; Cannady et al., 2018; Cannady et al., 2021). Notably, CIE did not affect other measures of the normalized GCaMP6f signal or the raw values, suggesting that the CIE-induced change in signaling is related to enhanced reward processing in PrL neurons. These effects of CIE on signaling surrounding ethanol drinking bouts appear specific to the PrL, at least when compared with the lateral orbitofrontal cortex, which did not reveal a change in the anticipatory signal in ethanol dependent mice (Gioia and Woodward, 2021). However, unlike PrL, CIE exposure increased frequency of GCaMP6f events in the OFC (Gioia and Woodward, 2021), demonstrating selective adaptations in frontal cortex after induction of ethanol dependence.

While our pre-bout data are consistent with an ‘intention to drink’ signal in the medial PFC of outbred Wistar rats (Linsenbardt et al., 2019), the intention signal after CIE markedly differs from that of alcohol-preferring (P) rats selectively bred for high ethanol drinking that are commonly used to study familial risk associated with AUD (McBride et al., 2014). The intention signal preceding ethanol drinking is blunted in P rats compared with Wistar rats and remains elevated in CIE exposed mice compared with air controls. These data suggest that genetics and induction of ethanol dependence exert aberrant control over

excessive drinking possibly through divergent signaling mechanisms in the PrL cortex. Although there are major differences between these two studies that could explain the differences in P rats and CIE-exposed mice (mice vs. rats; photometry vs single unit recordings; free access vs alcohol cues), we would argue that both studies provide evidence that aberrant signaling within the PrL cortex leads to excessive ethanol intake. Alternatively, it is possible that reorganization of other neural circuits or regions innervated by the PrL would show consistent neural firing patterns in CIE exposed mice and P rats that could explain the excessive drinking phenotype. Regardless, our study demonstrated an impaired intention signaling and altered response to quinine adulteration in the PrL cortex in ethanol dependent mice.

PrL→NAcore projection neurons

Contrary to our hypothesis, PrL→NAcore projection neurons did not encode for ethanol over water in a two-bottle choice home cage drinking model. While the overall signal surrounding licking bouts followed a similar pattern as the total PrL population, the signal in NAcore projecting PrL neurons for ethanol drinking bouts was equal to or lower than the signal for water bouts. Prolonged up-states in PrL→NAcore projection neurons also differed from the overall population in that up-state characteristics were similar with and without drinking bouts, demonstrating that the PrL→NAcore projection is encoding different aspects of hedonic value favoring water over ethanol when given a choice. Perhaps these findings are not surprising given the known role for the PrL cortex in controlling cue-induced reinstatement (Keistler et al., 2017) and compulsive-like ethanol drinking (Seif et al., 2013; Barbier et al., 2021). It is possible that ethanol dependence or a long history of excessive intake would produce an imbalance in excitation/inhibition processes that shift reward encoding toward ethanol over water in PrL→NAcore projections. Alternatively, other circuits, such as PrL→basolateral amygdala projections, might encode and drive excessive ethanol drinking in dependent mice (Barbier et al., 2021).

In summary, monitoring population calcium activity in PrL cortex identified an intention signal that varied with the perceived hedonic value of different drinking solutions and tracked changes in compulsive-like ethanol drinking in dependent mice. Multiple ML algorithms supported the encoding of reward salience across drinking solutions in the PrL cortical neurons under non-deprived recording conditions. We also observed differential encoding of water over ethanol in PrL neurons that project to the NAcore compared with population activity of the PrL cortex. Finally, we identified an aberrant intention signal in the PrL cortex that could serve as a mechanism driving excessive and compulsive-like ethanol drinking.

References

Amarante LM, Caetano MS, Laubach M (2017) Medial Frontal Theta Is Entrained to Rewarded Actions. J Neurosci 37:10757-10769.

Amiez C, Joseph JP, Procyk E (2006) Reward encoding in the monkey anterior cingulate cortex. Cereb Cortex 16:1040-1055.

Barbier E, Barchiesi R, Domi A, Chanthongdee K, Domi E, Augier G, Augier E, Xu L, Adermark L, Heilig M (2021) Downregulation of Synaptotagmin 1 in the Prelimbic Cortex Drives Alcohol-Associated Behaviors in Rats. Biol Psychiatry 89:398-406.

Barbier E, Tapocik JD, Juergens N, Pitcairn C, Borich A, Schank JR, Sun H, Schuebel K, Zhou Z, Yuan Q, Vendruscolo LF, Goldman D, Heilig M (2015) DNA methylation in the medial prefrontal cortex regulates alcohol-induced behavior and plasticity. J Neurosci 35:6153-6164.

Barbier E, Johnstone AL, Khomtchouk BB, Tapocik JD, Pitcairn C, Rehman F, Augier E, Borich A, Schank JR, Rienas CA, Van Booven DJ, Sun H, Natt D, Wahlestedt C, Heilig M (2017) Dependence-induced increase of alcohol self-administration and compulsive drinking mediated by the histone methyltransferase PRDM2. Mol Psychiatry 22:1746-1758.

Bates D, Mächler M, Bolker B, Walker S (2015) Fitting Linear Mixed-Effects Models Using lme4. Journal of Statistical Software 67:1 - 48.

Becker HC, Lopez MF (2004) Increased ethanol drinking after repeated chronic ethanol exposure and withdrawal experience in C57BL/6 mice. Alcohol Clin Exp Res 28:1829-1838.

Benjamin AS, Fernandes HL, Tomlinson T, Ramkumar P, VerSteeg C, Chowdhury RH, Miller LE, Kording KP (2018) Modern Machine Learning as a Benchmark for Fitting Neural Responses. Front Comput Neurosci 12:56.

Blaine SK, Wemm S, Fogelman N, Lacadie C, Seo D, Scheinost D, Sinha R (2020) Association of Prefrontal-Striatal Functional Pathology With Alcohol Abstinence Days at Treatment Initiation and Heavy Drinking After Treatment Initiation. Am J Psychiatry 177:1048-1059.

Boughter JD, Jr., Baird JP, Bryant J, St John SJ, Heck D (2007) C57BL/6J and DBA/2J mice vary in lick rate and ingestive microstructure. Genes Brain Behav 6:619-627.

Buschman TJ, Miller EK (2014) Goal-direction and top-down control. Philos Trans R Soc Lond B Biol Sci 369.

Calipari ES, Bagot RC, Purushothaman I, Davidson TJ, Yorgason JT, Pena CJ, Walker DM, Pirpinias ST, Guise KG, Ramakrishnan C, Deisseroth K, Nestler EJ (2016) In vivo imaging identifies temporal signature of D1 and D2 medium spiny neurons in cocaine reward. Proc Natl Acad Sci U S A 113:2726-2731.

Cannady R, Rinker JA, Nimitvilai S, Woodward JJ, Mulholland PJ (2018) Chronic Alcohol, Intrinsic Excitability, and Potassium Channels: Neuroadaptations and Drinking Behavior. Handb Exp Pharmacol 248:311-343.

Cannady R, Nguyen T, Padula AE, Rinker JA, Lopez MF, Becker HC, Woodward JJ, Mulholland PJ (2021) Interaction of chronic intermittent ethanol and repeated stress on structural and functional plasticity in the mouse medial prefrontal cortex. Neuropharmacology 182:108396.

Chen T, Guestrin CE (2016) XGBoost: A Scalable Tree Boosting System. In: Proceedings of the 22nd ACM SIGKDD International Conference on Knowledge Discovery and Data Mining, pp 785–794. San Francisco, California, USA: Association for Computing Machinery.

Davis JD, Smith GP (1992) Analysis of the microstructure of the rhythmic tongue movements of rats ingesting maltose and sucrose solutions. Behav Neurosci 106:217-228.

Emmons EB, De Corte BJ, Kim Y, Parker KL, Matell MS, Narayanan NS (2017) Rodent Medial Frontal Control of Temporal Processing in the Dorsomedial Striatum. J Neurosci 37:8718-8733.

Engleman EA, Ingraham CM, Rodd ZA, Murphy JM, McBride WJ, Ding ZM (2020) The reinforcing effects of ethanol within the prelimbic cortex and ethanol drinking: Involvement of local dopamine D(2) receptor-mediated neurotransmission. Drug Alcohol Depend 214:108165.

Frost ME, Peterson VL, Bird CW, McCool B, Hamilton DA (2019) Effects of Ethanol Exposure and Withdrawal on Neuronal Morphology in the Agranular Insular and Prelimbic Cortices: Relationship with Withdrawal-Related Structural Plasticity in the Nucleus Accumbens. Brain Sci 9.

Fuster JM (2015) The prefrontal cortex, Fifth edition. Edition. Amsterdam ; Boston: Elsevier/AP, Academic Press is an imprint of Elsevier.

Gioia DA, Woodward JJ (2021) Altered Activity of Lateral Orbitofrontal Cortex Neurons in Mice following Chronic Intermittent Ethanol Exposure. eNeuro 8.

Grucza RA, Sher KJ, Kerr WC, Krauss MJ, Lui CK, McDowell YE, Hartz S, Virdi G, Bierut LJ (2018) Trends in Adult Alcohol Use and Binge Drinking in the Early 21st-Century United States: A Meta-Analysis of 6 National Survey Series. Alcohol Clin Exp Res 42:1939-1950.

Gunaydin LA, Grosenick L, Finkelstein JC, Kauvar IV, Fenno LE, Adhikari A, Lammel S, Mirzabekov JJ, Airan RD, Zalocusky KA, Tye KM, Anikeeva P, Malenka RC, Deisseroth K (2014) Natural neural projection dynamics underlying social behavior. Cell 157:1535-1551.

Hasin DS, Stinson FS, Ogburn E, Grant BF (2007) Prevalence, correlates, disability, and comorbidity of DSM-IV alcohol abuse and dependence in the United States: results from the National Epidemiologic Survey on Alcohol and Related Conditions. Arch Gen Psychiatry 64:830-842.

Horst NK, Laubach M (2013) Reward-related activity in the medial prefrontal cortex is driven by consumption. Front Neurosci 7:56.

Hu W, Morris B, Carrasco A, Kroener S (2015) Effects of acamprosate on attentional set-shifting and cellular function in the prefrontal cortex of chronic alcohol-exposed mice. Alcohol Clin Exp Res 39:953-961.

Hughes BA, Bohnsack JP, O'Buckley TK, Herman MA, Morrow AL (2019) Chronic Ethanol Exposure and Withdrawal Impair Synaptic GABA(A) Receptor-Mediated Neurotransmission in Deep-Layer Prefrontal Cortex. Alcohol Clin Exp Res 43:822-832.

Hughes BA, Crofton EJ, O'Buckley TK, Herman MA, Morrow AL (2020) Chronic ethanol exposure alters prelimbic prefrontal cortical Fast-Spiking and Martinotti interneuron function with differential sex specificity in rat brain. Neuropharmacology 162:107805.

Jezzini A, Mazzucato L, La Camera G, Fontanini A (2013) Processing of hedonic and chemosensory features of taste in medial prefrontal and insular networks. J Neurosci 33:18966-18978.

Joffe ME, Winder DG, Conn PJ (2020) Contrasting sex-dependent adaptations to synaptic physiology and membrane properties of prefrontal cortex interneuron subtypes in a mouse model of binge drinking. Neuropharmacology 178:108126.

Joffe ME, Winder DG, Conn PJ (2021) Increased Synaptic Strength and mGlu(2/3) Receptor Plasticity on Mouse Prefrontal Cortex Intratelencephalic Pyramidal Cells Following Intermittent Access to Ethanol. Alcohol Clin Exp Res 45:518-529.

Johnson AW, Sherwood A, Smith DR, Wosiski-Kuhn M, Gallagher M, Holland PC (2010) An analysis of licking microstructure in three strains of mice. Appetite 54:320-330.

Keistler CR, Hammarlund E, Barker JM, Bond CW, DiLeone RJ, Pittenger C, Taylor JR (2017) Regulation of Alcohol Extinction and Cue-Induced Reinstatement by Specific Projections among Medial Prefrontal Cortex, Nucleus Accumbens, and Basolateral Amygdala. J Neurosci 37:4462-4471.

Klenowski PM, Fogarty MJ, Shariff M, Belmer A, Bellingham MC, Bartlett SE (2016) Increased Synaptic Excitation and Abnormal Dendritic Structure of Prefrontal Cortex Layer V Pyramidal Neurons following Prolonged Binge-Like Consumption of Ethanol. eNeuro 3.

Kroener S, Mulholland PJ, New NN, Gass JT, Becker HC, Chandler LJ (2012) Chronic alcohol exposure alters behavioral and synaptic plasticity of the rodent prefrontal cortex. PLoS One 7:e37541.

Kutlu MG, Zachry JE, Melugin PR, Cajigas SA, Chevee MF, Kelly SJ, Kutlu B, Tian L, Siciliano CA, Calipari ES (2021) Dopamine release in the nucleus accumbens core signals perceived saliency. Curr Biol 31:4748-4761 e4748.

Linsenbardt DN, Timme NM, Lapish CC (2019) Encoding of the Intent to Drink Alcohol by the Prefrontal Cortex Is Blunted in Rats with a Family History of Excessive Drinking. eNeuro 6.

Littell RC, Henry PR, Ammerman CB (1998) Statistical analysis of repeated measures data using SAS procedures. J Anim Sci 76:1216-1231.

Loeber S, Vollstadt-Klein S, von der Goltz C, Flor H, Mann K, Kiefer F (2009) Attentional bias in alcohol-dependent patients: the role of chronicity and executive functioning. Addict Biol 14:194-203.

Lopez MF, Becker HC (2005) Effect of pattern and number of chronic ethanol exposures on subsequent voluntary ethanol intake in C57BL/6J mice. Psychopharmacology (Berl) 181:688-696.

Lopez MF, Becker HC, Chandler LJ (2014) Repeated episodes of chronic intermittent ethanol promote insensitivity to devaluation of the reinforcing effect of ethanol. Alcohol 48:639-645.

Ma L, Hyman JM, Phillips AG, Seamans JK (2014) Tracking progress toward a goal in corticostriatal ensembles. J Neurosci 34:2244-2253.

McBride WJ, Rodd ZA, Bell RL, Lumeng L, Li TK (2014) The alcohol-preferring (P) and high-alcohol-drinking (HAD) rats--animal models of alcoholism. Alcohol 48:209-215.

McGuier NS, Padula AE, Lopez MF, Woodward JJ, Mulholland PJ (2015) Withdrawal from chronic intermittent alcohol exposure increases dendritic spine density in the lateral orbitofrontal cortex of mice. Alcohol 49:21-27.

Melendez RI, McGinty JF, Kalivas PW, Becker HC (2012) Brain region-specific gene expression changes after chronic intermittent ethanol exposure and early withdrawal in C57BL/6J mice. Addict Biol 17:351-364.

Meng C, Zhou J, Papaneri A, Peddada T, Xu K, Cui G (2018) Spectrally Resolved Fiber Photometry for Multi-component Analysis of Brain Circuits. Neuron 98:707-717 e704.

Moorman DE, James MH, McGlinchey EM, Aston-Jones G (2015) Differential roles of medial prefrontal subregions in the regulation of drug seeking. Brain Res 1628:130-146.

Mulholland PJ, Chandler LJ, Kalivas PW (2016) Signals from the Fourth Dimension Regulate Drug Relapse. Trends Neurosci 39:472-485.

Mulholland PJ, Teppen TL, Miller KM, Sexton HG, Pandey SC, Swartzwelder HS (2018) Donepezil Reverses Dendritic Spine Morphology Adaptations and Fmr1 Epigenetic Modifications in Hippocampus of Adult Rats After Adolescent Alcohol Exposure. Alcohol Clin Exp Res 42:706-717.

Nall RW, Heinsbroek JA, Nentwig TB, Kalivas PW, Bobadilla AC (2021) Circuit selectivity in drug versus natural reward seeking behaviors. J Neurochem 157:1450-1472.

Narayanan NS, Laubach M (2009) Delay activity in rodent frontal cortex during a simple reaction time task. J Neurophysiol 101:2859-2871.

Nash JC, Varadhan R (2011) Unifying Optimization Algorithms to Aid Software System Users: optimx for R. Journal of Statistical Software 43:1 - 14.

National Research Council (U.S.). Committee for the Update of the Guide for the Care and Use of Laboratory Animals., Institute for Laboratory Animal Research (U.S.), National Academies Press (U.S.) (2011) Guide for the care and use of laboratory animals. In, 8th Edition, pp xxv, 220 p. Washington, D.C.: National Academies Press,.

Padula AE, Griffin WC, 3rd, Lopez MF, Nimitvilai S, Cannady R, McGuier NS, Chesler EJ, Miles MF, Williams RW, Randall PK, Woodward JJ, Becker HC, Mulholland PJ (2015) KCNN Genes that Encode Small-Conductance Ca2+-Activated K+ Channels Influence Alcohol and Drug Addiction. Neuropsychopharmacology 40:1928-1939.

Palombo P, Leao RM, Bianchi PC, de Oliveira PEC, Planeta CDS, Cruz FC (2017) Inactivation of the Prelimbic Cortex Impairs the Context-Induced Reinstatement of Ethanol Seeking. Front Pharmacol 8:725.

Parent MA, Amarante LM, Liu B, Weikum D, Laubach M (2015) The medial prefrontal cortex is crucial for the maintenance of persistent licking and the expression of incentive contrast. Front Integr Neurosci 9:23.

Peters J, Kalivas PW, Quirk GJ (2009) Extinction circuits for fear and addiction overlap in prefrontal cortex. Learn Mem 16:279-288.

Petyko Z, Toth A, Szabo I, Galosi R, Lenard L (2009) Neuronal activity in rat medial prefrontal cortex during sucrose solution intake. Neuroreport 20:1235-1239.

Pfarr S, Meinhardt MW, Klee ML, Hansson AC, Vengeliene V, Schonig K, Bartsch D, Hope BT, Spanagel R, Sommer WH (2015) Losing Control: Excessive Alcohol Seeking after Selective Inactivation of Cue-Responsive Neurons in the Infralimbic Cortex. J Neurosci 35:10750-10761.

Pitel AL, Rivier J, Beaunieux H, Vabret F, Desgranges B, Eustache F (2009) Changes in the episodic memory and executive functions of abstinent and relapsed alcoholics over a 6-month period. Alcohol Clin Exp Res 33:490-498.

Pleil KE, Rinker JA, Lowery-Gionta EG, Mazzone CM, McCall NM, Kendra AM, Olson DP, Lowell BB, Grant KA, Thiele TE, Kash TL (2015a) NPY signaling inhibits extended amygdala CRF neurons to suppress binge alcohol drinking. Nat Neurosci 18:545-552.

Pleil KE, Lowery-Gionta EG, Crowley NA, Li C, Marcinkiewcz CA, Rose JH, McCall NM, Maldonado-Devincci AM, Morrow AL, Jones SR, Kash TL (2015b) Effects of chronic ethanol exposure on neuronal function in the prefrontal cortex and extended amygdala. Neuropharmacology 99:735-749.

Radke AK, Jury NJ, Kocharian A, Marcinkiewcz CA, Lowery-Gionta EG, Pleil KE, McElligott ZA, McKlveen JM, Kash TL, Holmes A (2017) Chronic EtOH effects on putative measures of compulsive behavior in mice. Addict Biol 22:423-434.

Renteria R, Cazares C, Gremel CM (2020) Habitual Ethanol Seeking and Licking Microstructure of Enhanced Ethanol Self-Administration in Ethanol-Dependent Mice. Alcohol Clin Exp Res 44:880-891.

Rhodes JS, Best K, Belknap JK, Finn DA, Crabbe JC (2005) Evaluation of a simple model of ethanol drinking to intoxication in C57BL/6J mice. Physiol Behav 84:53-63.

Rhodes JS, Ford MM, Yu CH, Brown LL, Finn DA, Garland T, Jr., Crabbe JC (2007) Mouse inbred strain differences in ethanol drinking to intoxication. Genes Brain Behav 6:1-18.

Rinker JA, Marshall SA, Mazzone CM, Lowery-Gionta EG, Gulati V, Pleil KE, Kash TL, Navarro M, Thiele TE (2017) Extended Amygdala to Ventral Tegmental Area Corticotropin-Releasing Factor Circuit Controls Binge Ethanol Intake. Biol Psychiatry 81:930-940.

Rossi F, Delannay N, Conan-Guez B, Verleysen M (2005) Representation of functional data in neural networks. Neurocomputing 64:183-210.

Samson HH, Chappell A (2001) Muscimol injected into the medial prefrontal cortex of the rat alters ethanol self-administration. Physiol Behav 74:581-587.

Schacht JP, Anton RF, Myrick H (2013) Functional neuroimaging studies of alcohol cue reactivity: a quantitative meta-analysis and systematic review. Addict Biol 18:121-133.

Seamans JK, Nogueira L, Lavin A (2003) Synaptic basis of persistent activity in prefrontal cortex in vivo and in organotypic cultures. Cereb Cortex 13:1242-1250.

Seif T, Chang SJ, Simms JA, Gibb SL, Dadgar J, Chen BT, Harvey BK, Ron D, Messing RO, Bonci A, Hopf FW (2013) Cortical activation of accumbens hyperpolarization-active NMDARs mediates aversion-resistant alcohol intake. Nat Neurosci 16:1094-1100.

Siciliano CA, Noamany H, Chang CJ, Brown AR, Chen X, Leible D, Lee JJ, Wang J, Vernon AN, Vander Weele CM, Kimchi EY, Heiman M, Tye KM (2019) A cortical-brainstem circuit predicts and governs compulsive alcohol drinking. Science 366:1008-1012.

Stavro K, Pelletier J, Potvin S (2013) Widespread and sustained cognitive deficits in alcoholism: a meta-analysis. Addict Biol 18:203-213.

Steinmetz NA, Zatka-Haas P, Carandini M, Harris KD (2019) Distributed coding of choice, action and engagement across the mouse brain. Nature 576:266-273.

Steinmetz NA et al. (2017) Aberrant Cortical Activity in Multiple GCaMP6-Expressing Transgenic Mouse Lines. eNeuro 4.

Trantham-Davidson H, Burnett EJ, Gass JT, Lopez MF, Mulholland PJ, Centanni SW, Floresco SB, Chandler LJ (2014) Chronic alcohol disrupts dopamine receptor activity and the cognitive function of the medial prefrontal cortex. J Neurosci 34:3706-3718.

Varodayan FP, Sidhu H, Kreifeldt M, Roberto M, Contet C (2018) Morphological and functional evidence of increased excitatory signaling in the prelimbic cortex during ethanol withdrawal. Neuropharmacology 133:470-480.